

## October 2002 30-day incoherent scatter radar experiments at Millstone Hill and Svalbard and simultaneous GUVI/TIMED observations

Shun-Rong Zhang,<sup>1</sup> John M. Holt,<sup>1</sup> Phil J. Erickson,<sup>1</sup> Frank D. Lind,<sup>1</sup> John C. Foster,<sup>1</sup> Anthony P. van Eyken,<sup>2</sup> Yongliang Zhang,<sup>3</sup> Larry J. Paxton,<sup>3</sup> William C. Rideout,<sup>1</sup> Larisa P. Goncharenko,<sup>1</sup> and Glenn R. Campbell<sup>1</sup>

Received 11 June 2004; revised 19 November 2004; accepted 10 December 2004; published 15 January 2005.

[1] A long-duration incoherent scatter radar (ISR) experiment was conducted at Millstone Hill and Svalbard from October 4–November 4, 2002. Along with the simultaneous GUVI/TIMED neutral composition measurements, this 30-day run enabled us to study a number of thermosphere-ionosphere-magnetosphere phenomena. This paper focuses on the day-to-day variability and quasiperiodic oscillation of the ionosphere. The day-to-day variability under quiet magnetic conditions in electron density  $N_e$ , ion temperature  $T_i$  and electron temperature  $T_e$ , respectively, changed with local time and height, with the largest variability in  $N_e$  and the smallest in  $T_i$ . Midnight through dawn was the period of largest variability. Quasiperiodic  $N_e$  oscillations were present with periods  $>1$  day. Some of these oscillations were correlated with changes in the neutral composition originating from geomagnetic activity, which altered the global atmospheric circulation as a result of high latitude heating processes as indicated in Svalbard ion temperature enhancements. However, the wave-type oscillation of  $N_e$  exhibits a downward phase progression which persists up to 600 km and prevails until a large storm appears to impose an upward phase progression. **Citation:** Zhang, S.-R., et al. (2005), October 2002 30-day incoherent scatter radar experiments at Millstone Hill and Svalbard and simultaneous GUVI/TIMED observations, *Geophys. Res. Lett.*, 32, L01108, doi:10.1029/2004GL020732.

### 1. Introduction

[2] From October 4 to November 4, 2002, a 32 consecutive day incoherent scatter radar (ISR) campaign was conducted by the EISCAT Svalbard Radar (ESR) and the Millstone Hill Radar. This experiment, which was the longest ever attempted by incoherent scatter radars (compared to a typical  $\leq 5$ -day operation), provided a unique opportunity to study many important ionosphere-thermosphere phenomena, e.g., the ionospheric variability [Forbes *et al.*, 2000; Rishbeth and Mendillo, 2001] and long-lasting space weather events. This experiment covered both geomagnetically quiet and

active periods, facilitating theoretical model testing and validation. Day-to-day ionospheric oscillations [Forbes and Zhang, 1997; Altadill and Apostolov, 2001; Pancheva *et al.*, 2002] may also be studied through analyses of this long and continuous time series of data. The global neutral atmosphere was simultaneously monitored by the TIMED spacecraft in a 625 km circular orbit above Earth. The Global Ultraviolet Imager (GUVI) instrument onboard the spacecraft produces far-ultraviolet imaging spectrograms of photons emitted from the upper atmosphere, providing dayside neutral composition information [see, e.g., Christensen *et al.*, 2003].

[3] This paper presents results from both radars and from the TIMED/GUVI instrument. We focus on the ionospheric day-to-day variability and oscillation and their changes with altitude under quiet and active magnetic conditions.

### 2. 30-Day ISR Experiments

[4] At Millstone Hill (42.6°N, 288.5°E, Invariant Lat. 53.4°) a 68-m zenith antenna was used to continuously measure electron density  $N_e$ , electron temperature  $T_e$ , ion temperature  $T_i$ , and line-of-sight velocity  $V_o$  with interleaved single pulses and alternating-coded pulses. The data integration time was 4 min. For the EISCAT Svalbard radar (78.1°N, 16.0°E, Invariant Lat. 75.1°), the CP2 program was used for most of the experiment with the fixed geomagnetic field aligned antenna, and the steerable antenna was pointed vertically as well as toward the east and the west of the field. For this study we use only the fixed field-aligned data.

### 3. Solar-Geophysical Conditions

[5] The daily solar 10.7 cm radio flux index F107, hourly Dst index, and 3-hourly ap index are shown in Figure 1. F107 varied between 135 to 180 units from October 4 to November 4, 2002 (day numbers 277–308), whereas its 81-day average was around 175 units and tended to decrease. The index, which was larger near the middle of the month, also showed a gradual change with a 27-day periodicity, which originated from the solar synodic rotation. October 21 (day 294) may be set as a good reference day, since F107 did not change in the previous two days and magnetic activity was very quiet on that day as well as the prior 3 days. Magnetic disturbances were noticeable on three occasions: on day 280 Dst dropped to  $-100$  nT where it stayed for about 1 full day before it recovered; on day 287 a sharp and brief drop in Dst occurred; on October 24 (day 297), a major storm was

<sup>1</sup>Haystack Observatory, Massachusetts Institute of Technology, Westford, Massachusetts, USA.

<sup>2</sup>European Incoherent Scatter (EISCAT) Scientific Association, Kiruna, Sweden.

<sup>3</sup>Johns Hopkins University Applied Physics Laboratory, Laurel, Maryland, USA.

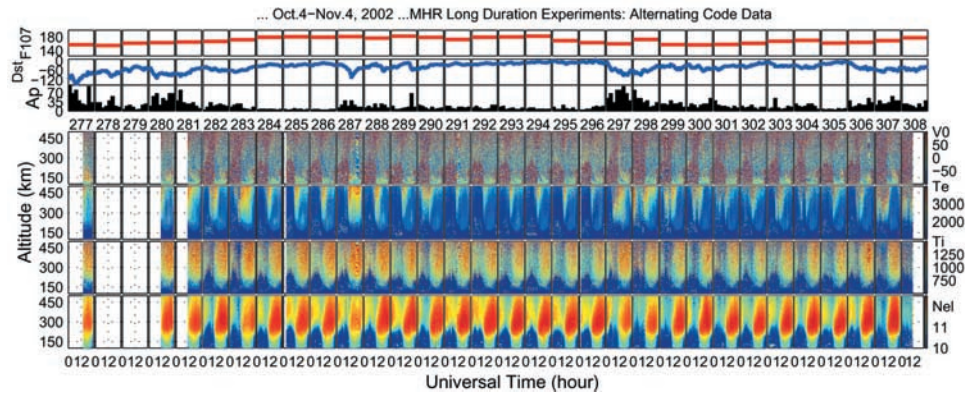


**Figure 1.** Millstone Hill alternating code data between October 4 and November 4, 2002 of electron density (in log10 scale for a density unit  $\text{m}^{-3}$ ), ion and electron temperatures (K), and vertical ion velocity (m/s). Solar geophysical indices are the daily solar 10.7 cm flux F107, the hourly Dst index, and the 3-hourly ap index.

launched with a Dst main phase of 12 hours and recovery phase of several days, causing severe ionospheric storms.

#### 4. Variation Pattern and Quiet-Time Variability

[6] Figure 1 also shows the whole set of alternating-code ISR data for Millstone Hill. The day-to-day changes can be seen clearly even for quiet geomagnetic conditions. The variability was recently discussed by *Rishbeth and Mendillo* [2001] based on long-term F2 peak data. Our ISR Ne variability (defined quantitatively as standard deviations divided by averages), as shown in Figure 2 for  $ap < 10$ , tended to maximize about 100 km above the peak, although the maximum absolute variability (standard deviation of the average) is present near the peak, suggesting the significance of non-chemical processes. Chemical composition effects contribute to the Ne variability in the F2 region through changes in the O/N2 ratio which can be significant even under quiet conditions (next section). Non-chemical causes include dynamical changes of vertical ion motions (next section) induced by winds and  $\mathbf{E} \times \mathbf{B}$  drifts; e.g., *Mendillo et al.* [2002] suggested the wind variability effect on the ionospheric variability. Another interesting cause is tides and waves in the mesosphere/lower thermosphere (MLT) region which can be dynamically coupled upward to generate ionospheric perturbations and long period oscillations [*Forbes et al.*, 1993]. We will discuss the quasiperiodic ionospheric oscillations observed during the 30-day run in the next section.

[7] The variability in Te is smaller than that in Ne. Due to the strong anti-correlation between Ne and Te [*Schunk and Nagy*, 1978; *Zhang et al.*, 2004] which can be seen in Figure 1, the very variable Ne near the F2 peak can lead to more variability in Te there. As for Ti, the magnetospheric heat flux contributes to the temperature increase at high altitudes. Therefore, changes in the ion heat flux, along with the Te variability and ion-electron energy coupling, may cause Ti variability increase with height. At low altitudes however, since ions are in close thermal contact with neutrals whose temperature is less variable, Ti exhibits less variability than Te and Ne.

[8] The variability in Ne and Te was larger from local midnight through dawn than during other periods. Calcula-

tions for Millstone Hill indicate that the magnetic conjugate ionosphere ( $>100$  km) sunrise occurred between the Millstone Hill midnight and sunrise through day 297, thus effects of photoelectrons from the conjugate ionosphere could lead to much of the observed variability.

[9] For Svalbard, the average diurnal variation (Figure 3 for  $ap < 10$ ) in Ne was characterized by two maxima, one around 0900 UT (10 SLT or 12 Magnetic LT) when the radar is in the dayside cusp and photoionization is strong, and a secondary one around 1900 UT when the so-called “Universal Time Effect” of the polar ionosphere was present. The effect has been explained in terms of the neutral wind that blows across the magnetic pole toward the geographic pole [*King et al.*, 1968]. This latter maximum in the nightside experiences more variability than the maximum in the sunlit dayside. The variability (see error bars representing standard deviations) in the three parameters, especially in Ti, was more drastic than for Millstone Hill due to the frequent particle precipitation and various heating processes originating from the magnetosphere. The

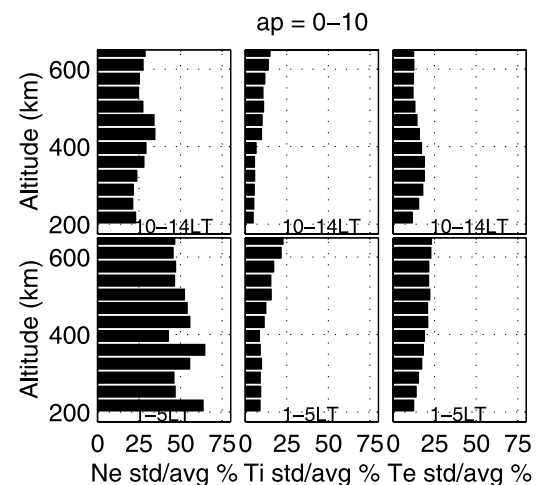


**Figure 2.** Variability (standard deviation over average) in Ne, Ti and Te during 10–14LT (upper) and 1–5LT (bottom) for quiet conditions ( $ap < 10$ ) at Millstone Hill. The radar single pulse data were used.

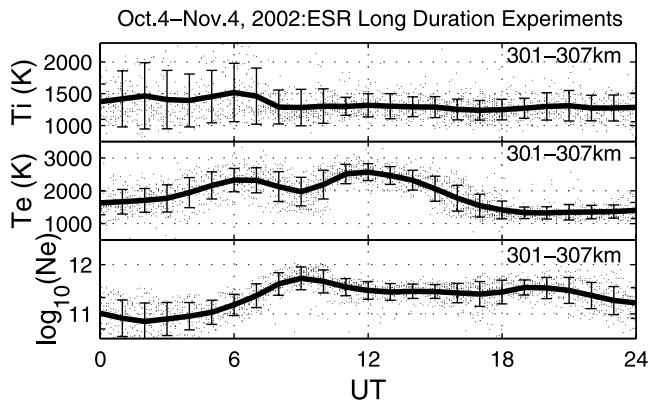


**Figure 3.** ESR data points and hourly averages with  $ap < 10$  around 300 km during October 4 and November 4, 2002 for electron density (in  $\log_{10}$  scale for a density unit  $\text{m}^{-3}$ ), ion and electron temperatures. Error bars represent the standard deviation of the averages. Local noon is around 11 UT.

electron temperature  $T_e$  reached a minimum around 0900 UT as a result of the high Ne.

## 5. Day-to-Day Oscillation

[10] As mentioned earlier, some of the ionospheric variability may result from long period ionospheric oscillations. To examine the day-to-day oscillation, it is desirable to remove the diurnal and higher frequency components in the data. Our approach was to compute the hourly binned average, de-trend the average over the 30 days, run through a low-pass filter with a band-width of 3 days, and compute a 24-hour running average. Results from this procedure for both sites are shown in Figure 4, along with the daytime GUVI column  $O/N_2$ . The TIMED satellite flies over Millstone Hill at a local time which shifts daily by 20 min. Uncertainty in the  $O/N_2$  data is expected to be less than 10% for lower  $O/N_2$  values and latitudes below polar regions. Ne was low before day 284 (more data before day 284 were obtained with the single pulse observations), followed by a period of high Ne for 11 days. It then returned back to a low level. Ne was generally higher between days 284–296 than in other days, perhaps mirroring a stronger EUV flux during the 27-day cycle of the solar rotation.

[11] The F2 region  $O^+$  is largely produced through O photoionization and loss to  $N_2$ , so chemical processes make Ne proportional to  $O/N_2$ . Ne was low (10~20% below the trend line for the 30 days) on days 283 and 287–288, decreased dramatically between days 297–299 (~40% below the reference trend) when the long-lasting Dst drop was present, and was low again on day 302. These Ne decreases correlated well with the corresponding  $O/N_2$  drops. Around day 292, however, there appeared a high Ne but no significant  $O/N_2$  increase, suggesting possible non-chemical effects.

[12] Vertical ion drifts, filtered and averaged in the same manner as Ne, exhibit day-to-day fluctuations, with downward drifts largely corresponding to low Ne. The meridional wind is an important contributor to the drift. The southward wind, which can be strengthened during storms and substorms, drives ions downward along the field line through the drag force to altitudes where the ion loss rate is higher,

and carries the neutral constituents which have a low  $O/N_2$  ratio, away from the magnetic pole in the global circulation. These direct and indirect effects on the local ionosphere, which were recently discussed by Kawamura *et al.* [2002], need to be carefully examined in the future with Millstone Hill radar steerable antenna experiments which can provide reliable wind estimates.

[13] High latitude heating is an important driver of global neutral atmospheric circulations [Fuller-Rowell *et al.*, 1996]. As a good indicator of various heating processes due to precipitating particles, enhanced electric fields, etc., high Ti values were observed by the ESR on days 281–282, 287–288, 297–298, 300, and 291 (for high altitudes). These high Ti days coincided well with those for Millstone Hill, and with drops in  $O/N_2$ , vertical drifts, and Ne. During large storms (days 297–298) the Ti increase appeared prior to the Ne decrease. It could be caused by the electric field enhancement which occurred prior to the onset of the Ne decrease in the storm main phase. The simultaneous appearance of high Ti over Svalbard and Millstone Hill does not necessarily mean the increases were caused by the same electric field source. Localized electric fields, such as the Sub-Auroral Polarization Stream associated fields [Foster and Vo, 2002], could give rise to the Ti enhancement over Millstone Hill.

[14] The wave-type >1 day oscillations in Ne have clear phase propagations, as shown by white curves in Figure 4 which run through local maximum or minimum Ne on the time axis at various heights. Around day 292, the phase at the topside is at least 8 hours earlier than at the bottomside, and the elevated Ne does not seem to be correlated with any obvious geomagnetic conditions. It might be possible, however, that this feature is associated with the vertical propagation of large scale MLT waves such as the 2-day

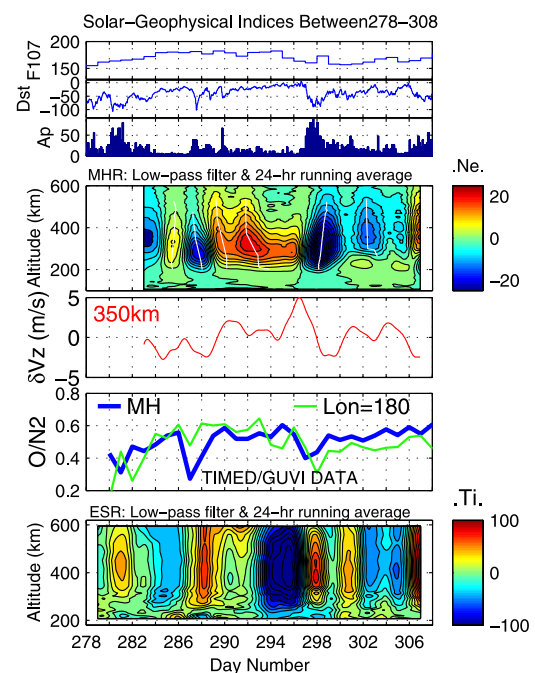


**Figure 4.** Ionospheric oscillations as derived from the ISR electron density (in unit  $10^{12} \text{m}^{-3}$ ) and vertical ion drifts at 350 km at Millstone Hill, the ISR ion temperature at Svalbard, and the GUVI column  $O/N_2$  for Millstone Hill as well as to the west of the observatory.

planetary wave [Forbes and Zhang, 1997]. Altadill and Apostolov [2001] have identified such propagating signatures from ionosonde bottomside Ne profiles between 170–230 km, and evaluated several mechanisms for the downward or upward wave progression. The downward phase, as shown here, persists up to 600 km and seems to prevail during most of our experiments. It was interrupted during the severe ionospheric storm commencing on day 297, where Ne was greatly reduced and the decrease began earlier at low altitudes than at high ones (upward phase). Geomagnetic forcing alters not only the ionosphere but also the lower atmosphere in terms of the tidal pattern of winds [Balan et al., 2004; Goncharenko et al., 2004]. We note that simultaneous MLT data are very critical to confirm the wave effects in the ionosphere. Indeed, simultaneous observations in the MLT, thermosphere and ionosphere regions, such as reported by Balan et al. [2004] for a 10-day campaign in Japan covering magnetically quiet and highly active conditions, will provide solid evidence for the MLT impact on the ionospheric variability and oscillations. It is also important to develop sophisticated techniques in order to characterize the waves and elaborate the roles of chemistry and dynamics observed in long-duration ISR experiments.

## 6. Summary

[15] 30-day ISR experiments were conducted from October 4 to November 4, 2002 at Millstone Hill and Svalbard. Data from this long-duration experiment, along with the simultaneous GUVI/TIMED data, enabled us to study many thermosphere-ionosphere-magnetosphere phenomena.

[16] This paper has focused on the ionospheric day-to-day variability and quasiperiodic oscillation, and the relevant chemistry and dynamics. The day-to-day variability under quiet magnetic conditions in Ne, Ti, and Te, respectively, changed with local time and height, with the largest variability in Ne and the smallest in Ti. The Ne and Ti variability tended to increase with height while the Te variability was relatively large slightly above the F2 peak. Midnight through dawn was the period of largest variability. Quasiperiodic oscillations in Ne were present with periods >1 day. Some of these oscillations were correlated with changes in the neutral composition originating from geomagnetic activity, which altered the global atmospheric circulation as a result of high latitude heating processes as indicated in enhancements of the Svalbard ion temperature. However, the wave-type oscillation of Ne exhibits a downward phase progression which persists up to 600 km and prevails over the experiment until a large storm appears to impose an upward phase progression.

[17] **Acknowledgments.** The Millstone Hill incoherent scatter radar is supported by a cooperative agreement between the National Science

Foundation and the Massachusetts Institute of Technology. EISCAT is an international association supported by the research councils of Finland (SA), France (CNRS), the Federal Republic of Germany (MPG), Japan (NIPR), Norway (NFR), Sweden (VR) and the United Kingdom (PPARC).

## References

- Altadill, D., and E. M. Apostolov (2001), Vertical propagating signatures of wave-type oscillations (2- and 6.5-days) in the ionosphere obtained from electron-density profiles, *J. Atmos. Sol. Terr. Phys.*, *63*, 823–834.
- Balan, N., et al. (2004), Simultaneous mesosphere/lower thermosphere and thermospheric F region observations during geomagnetic storms, *J. Geophys. Res.*, *109*, A04308, doi:10.1029/2003JA009982.
- Christensen, A. B., et al. (2003), Initial observations with the Global Ultraviolet Imager (GUVI) in the NASA TIMED satellite mission, *J. Geophys. Res.*, *108*, 1451, doi:10.1029/2003JA009918.
- Forbes, J. M., and X. Zhang (1997), Quasi 2-day oscillation of the ionosphere: A statistical study, *J. Atmos. Sol. Terr. Phys.*, *59*, 1025–1034.
- Forbes, J. M., R. G. Roble, and C. G. Fesen (1993), Acceleration, heating, and compositional mixing of the thermosphere due to upward propagating tides, *J. Geophys. Res.*, *98*, 311–321.
- Forbes, J. M., S. E. Palo, and X. Zhang (2000), Variability of the ionosphere, *J. Atmos. Sol. Terr. Phys.*, *62*, 685–693.
- Foster, J. C., and H. B. Vo (2002), Average characteristics and activity dependence of the subauroral polarization stream, *J. Geophys. Res.*, *107*(A12), 1475, doi:10.1029/2002JA009409.
- Fuller-Rowell, T. J., M. V. Codrescu, H. Rishbeth, R. J. Moffett, and S. Quegan (1996), On the seasonal response of the thermosphere and ionosphere to geomagnetic storms, *J. Geophys. Res.*, *101*, 2343–2353.
- Goncharenko, L. P., J. E. Salah, J. C. Foster, and C. Huang (2004), Variations in lower thermosphere dynamics at midlatitudes during intense geomagnetic storms, *J. Geophys. Res.*, *109*, A04304, doi:10.1029/2003JA010244.
- Kawamura, S., N. Balan, Y. Otsuka, and S. Fukao (2002), Annual and semiannual variations of the midlatitude ionosphere under low solar activity, *J. Geophys. Res.*, *107*(A8), 1166, doi:10.1029/2001JA000267.
- King, J. W., H. Kohl, D. M. Preece, and C. Seabrook (1968), An explanation of phenomena occurring in the high-latitude ionosphere at certain universal times, *J. Atmos. Sol. Terr. Phys.*, *30*, 11–23.
- Mendillo, M., H. Rishbeth, R. G. Roble, and J. Wroten (2002), Modeling F2-layer seasonal trends and day-to-day variability driven by coupling with the lower atmosphere, *J. Atmos. Sol. Terr. Phys.*, *64*, 1911–1931.
- Pancheva, D., M. Mitchell, B. R. Clark, J. Drobjeva, and J. Lastovicka (2002), Variability in the maximum height of the ionospheric F2-layer over Millstone Hill (September 1998–March 2000): Influence from below and above, *Ann. Geophys.*, *20*, 1807–1819.
- Rishbeth, H., and M. Mendillo (2001), Patterns of F2-layer variability, *J. Atmos. Sol. Terr. Phys.*, *63*, 1661–1680.
- Schunk, R. W., and A. F. Nagy (1978), Electron temperatures in the F region ionosphere: Theory and observations, *Rev. Geophys.*, *16*, 355–399.
- Zhang, S.-R., J. M. Holt, A. M. Zalucha, and C. Amory-Mazaudier (2004), Midlatitude ionospheric plasma temperature climatology and empirical model based on Saint Santin incoherent scatter radar data from 1966 to 1987, *J. Geophys. Res.*, *109*, A11311, doi:10.1029/2004JA010709.

G. R. Campbell, P. J. Erickson, J. C. Foster, L. P. Goncharenko, J. M. Holt, F. D. Lind, W. C. Rideout, and S.-R. Zhang, Haystack Observatory, MIT, Route 40, Westford, MA 01886, USA. (grc@haystack.mit.edu; pje@haystack.mit.edu; jcf@haystack.mit.edu; lpg@haystack.mit.edu; jmh@haystack.mit.edu; flind@haystack.mit.edu; brideout@haystack.mit.edu; shunrong@haystack.mit.edu)

L. J. Paxton and Y. Zhang, Johns Hopkins University Applied Physics Laboratory, 11100 Johns Hopkins Road, Laurel, MD 20723, USA. (larry.paxton@jhuapl.edu; yongliang.zhang@jhuapl.edu)

A. P. van Eyken, EISCAT Scientific Association, P.O. Box 164, SE-981 23 Kiruna, Sweden. (tony.van.eyken@eiscat.com)